2024 European Control Conference (ECC)
June 25-28, 2024. Stockholm, Sweden

Trotting gait optimization method for a quadruped robot

Alessandro Zanotti[1], Maicol Laurenza[1], Gianluca Pepe[1] and Antonio Carcaterra[1]

Abstract — **The quadruped robots represent a rapidly growing field in the industrial world due to their various applications in supporting everyday and hazardous human activities. Despite significant research contributions, gait optimization remains a challenging task. Typically, gait patterns are inspired by mimicking nature but fall short of replicating the flexibility and articulated adaptability observed in animals. This paper introduces a new method for optimizing gait and designing quadruped robots offline. This approach takes into account the dynamics of the entire system, including leg masses, by employing genetic algorithms and nonlinear programming techniques. The results of this new technique enable the exploration of gait patterns that can accommodate the rigidity of robots while minimizing the energy cost of locomotion.**

I. INTRODUCTION

Quadruped robots, also known as four-legged robots, represent a fascinating and rapidly evolving field within robotics. These machines, inspired by the locomotion of animals like dogs, cheetahs, and horses, have garnered significant interest for their ability to navigate diverse and challenging environments. Unlike their bipedal counterparts, quadruped robots possess intrinsic stability and versatility that make them suitable for a wide range of applications.

The study of quadruped locomotion has drawn researchers from various disciplines, driving advancements in mechanics, control systems, and materials science. These collective efforts have led to the development of sophisticated robots capable of executing precise and dynamic movements, even on rough terrains [1-5]. In recent years, quadruped robots have transitioned from experimental prototypes to practical real-world applications. They have found use in sectors such as research and rescue, agriculture, exploration, and logistics. Furthermore, their ability to navigate difficult environments with agility and endurance has opened the door to applications in disaster relief and environmental monitoring [6-8].

Despite significant progress, challenges persist in optimizing gait types and locomotion control [9]. Researchers are actively exploring innovative approaches, such as advanced optimization models [10-13] predictive control systems [14], and the integration of flexible elements [15-18], to enhance performance and adaptability.

Among the various optimization and control methodologies, those that generate robust gaits while simultaneously minimizing the energy cost of locomotion are of particular relevance. It is known from the literature that as transport speeds increase [10, 11, 15], it is advantageous to change the gait in order to minimize the energy cost. Thus, transitions occur from walking to a walking trot at low speeds, which have clear support polygons and are easily controllable, to a flying trot and gallop at high speeds, which have support lines or even intermittent support points interspersed with flight phases. However, while changing gaits at high speeds is beneficial, it becomes increasingly complex to control these systems and ensure their stability and periodicity of motion.

Currently, trajectory optimization techniques are based on important assumptions such as lightweight or even negligible legs, along with motion solutions derived from the simplified Single Rigid Body - SRB model [1, 2, 10, 15]. Applications on real robots are predominantly based on Central Pattern Generators for gaits like walking and walking trot [19]. These gaits have the advantage of being supported by support polygons and based on Zero Hybrid Dynamics [20], typically very robust. Conversely, systems that are inherently more unstable with support lines and jumps require predictive feedback controls capable of accounting for the strong nonlinearities of the system [17, 18, 21].

In this paper, we propose an innovative approach to generating optimized gaits with the dual objectives of reducing the energy Cost of Transport - CoT and eliminating the dynamic residuals associated with the presence of inertial legs. The algorithm has been designed in such a way that, through a series of iterative sub-optimizations, it manages to identify a closed and periodic solution capable of satisfying the motion equations of the robot. However, it is worth noting that this process does not occur in real-time but takes a few minutes to ensure convergence towards an optimal and compatible solution. The gait generator is based on the evolutionary algorithm, Genetic Algorithm - GA, as presented in [10], but here, it is enhanced to introduce new and crucial elements. In this algorithm: (i) it incorporates the yaw equation, allowing for a more comprehensive understanding of the robot's rotational dynamics; (ii) it includes a concept of a "dummy leg" within the optimization cycle, which accurately approximates the overall dynamics; (iii) it resolves contact forces in a way that absorbs all the inertial residuals of the complete multi-body system.

To demonstrate the effectiveness of this approach, we present the solution for the trot gait, which is characterized by the absence of a support polygon. Furthermore, to highlight

Manuscript received November 6, 2023. [1]The authors are with the Department of Mechanical and Aerospace Engineering of the University "La Sapienza" of Rome (e-mail: alessandro.zanotti@uniroma1.it,).

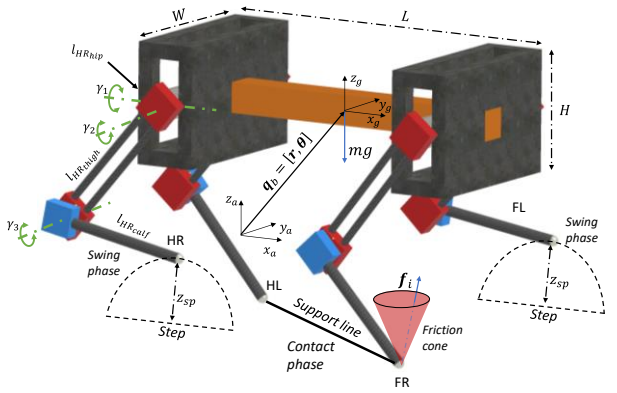

Figure 1: Schematic representation of the robotic system.

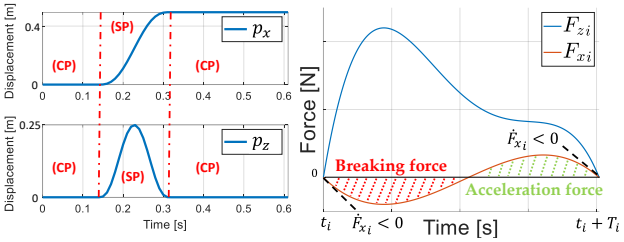

Figure 2: On the left: foot trajectory $p(t)$ along x and z directions. On the right: normal and longitudinal ground forces F_{z_i}, F_{x_i}, with $\dot{F}_{x_i}(t_i) < 0$ for incipient contact and $\dot{F}_{x_i}(t_i + T_i) < 0$ for the foot detachment, in accordance with the typical behavior of animals observed in nature.

the capabilities of the method that takes into account a significant leg mass compared to the body, we have identified a gait that significantly raises the tips of the feet, thus simulating the overcoming of terrain obstacles while simultaneously minimizing the CoT.

The article is divided into three sections: the first section introduces the motion equations of the quadruped robot and the SRB model with a dummy leg. The second section describes the optimization algorithm. Finally, in the third section, the trot results are presented, comparing them with the results obtained using the SRB model with non-"negligible" leg masses.

I. Mathematical Model for the Gait Optimization

A. Robot's gait parameters

The Figure 1 describes the robotic system under consideration. The robot is composed of a rigid trunk and four legs identified by the index $i = FR, HR, FL, HL$ representing front right, hind right, front left, and hind left legs respectively. The legs interact with the ground to determine the motion of the robot. Each leg has a contact phase (CP) during which it interacts with the ground and a swing phase (SP) to move towards the next contact point. For stable motion of the robot, the sequence of the CP and SP of each leg must produce a globally periodic motion of period T. To identify a specific gait of the robot, the parameters $t_i \in [0, T]$ and T_i representing the time at which each leg meets the ground and the time duration of the CP, respectively, must be known. The ratio between these two quantities is typically referred to as the duty factor $\beta_i = \frac{T_i}{T}$, which is a dimensionless parameter characterizing the gait of quadrupeds.

B. Quadrupedal model with dummy legs

The motion equations of an 18 degrees of freedom quadruped robot, as shown in the Figure 1, allowing leg adduction and rotation of the thigh and knee, can be described in a compact form:

$$\boldsymbol{M}(\boldsymbol{q})\ddot{\boldsymbol{q}} + \boldsymbol{C}(\boldsymbol{q}, \dot{\boldsymbol{q}})\dot{\boldsymbol{q}} = \boldsymbol{S}\boldsymbol{\tau} + \boldsymbol{g}(\boldsymbol{q}) + \boldsymbol{J}(\boldsymbol{q})^T\boldsymbol{f} \qquad (1)$$

where the state vector $\boldsymbol{q} = [\boldsymbol{q}_b, \boldsymbol{q}_l]^T$ is organized in two groups:

1. the body coordinates $\boldsymbol{q}_b = [\boldsymbol{r}, \boldsymbol{\theta}]^T$ composed by the position vector of the centre of gravity $\boldsymbol{r} = [x, y, z]^T$ with respect the fixed reference frame and the three angles roll, pitch and yaw $\boldsymbol{\theta} = [\theta, \phi, \psi]^T$ between the fixed and mobile reference frames;
2. the $n = 12$ −leg's joint variables $\boldsymbol{q}_l = [\gamma_1, \dots, \gamma_n]^T$.

Then, $\boldsymbol{M}, \boldsymbol{C} \in \mathbb{R}^{(6+n)\times(6+n)}$ are the mass and centrifugal-Coriolis matrixes; $\boldsymbol{S} = [\boldsymbol{0}_{n\times 6} \quad \boldsymbol{I}_{n\times n}]^T$ is the selection matrix of the n −leg's actions torque $\boldsymbol{\tau}$; $\boldsymbol{g} \in \mathbb{R}^{6+n}$ is the gravity force; $\boldsymbol{J}(\boldsymbol{q})^T \in \mathbb{R}^{(6+n)\times m}$ is the Jacobian of the $m = 4$ −ground forces $\boldsymbol{f} = \sum \boldsymbol{f}_i$ with $\boldsymbol{f}_i = [F_{xi}, F_{yi}, F_{zi}]$.

The primary goal of this research is to determine the trajectory $\boldsymbol{q}$ that aligns with the gait parameters selected by the GA algorithm described in the following section and simultaneously satisfies the motion equations (1) while minimizing CoT. However, fully addressing this problem can be challenging, as explained in [10, 11], due to significant discontinuities occurring when the foot tips initially contact the ground, the potential for multiple solutions, and configurations that are not achievable kinematically. For these reasons, we approach the problem in stages, identifying intermediate solutions that initially adhere to simplified models and then adapting them to the comprehensive model. Below, we illustrate how the optimization algorithm is constructed, starting with the SRB combined with a simplified dynamic model of the legs, which allows us to generate candidate solutions and subsequently complete the resolution of the global problem, thereby eliminating any remaining dynamic residuals.

Splitting the equation (1) and isolating the 6 body's DoF, is possible to explicit the inertia contributions that the legs act on the body $\boldsymbol{\mathcal{R}}_b$ and vice versa $\boldsymbol{\mathcal{R}}_l$ as:

$$\begin{aligned} \boldsymbol{M}_b(\boldsymbol{q})\ddot{\boldsymbol{q}}_b + \boldsymbol{C}_b(\boldsymbol{q}, \dot{\boldsymbol{q}})\dot{\boldsymbol{q}}_b \\ = \boldsymbol{g}_b(\boldsymbol{q}_b) + \boldsymbol{J}_b(\boldsymbol{q})^T\boldsymbol{f} \\ + \boldsymbol{\mathcal{R}}_b(\boldsymbol{q}, \dot{\boldsymbol{q}}, \ddot{\boldsymbol{q}}_l) \end{aligned} \qquad (2)$$

$$\begin{aligned} \boldsymbol{M}_l(\boldsymbol{q})\ddot{\boldsymbol{q}}_l + \boldsymbol{C}_l(\boldsymbol{q}, \dot{\boldsymbol{q}})\dot{\boldsymbol{q}}_l \\ = \boldsymbol{g}_l(\boldsymbol{q}) + \boldsymbol{J}_l(\boldsymbol{q})^T\boldsymbol{f} + \boldsymbol{\tau} \\ + \boldsymbol{\mathcal{R}}_l(\boldsymbol{q}, \dot{\boldsymbol{q}}, \ddot{\boldsymbol{q}}_b) \end{aligned} \qquad (3)$$

At this point, is possible to rewrite (2) in a compact form explicating the translational and rotational contributions:

$$m\ddot{\boldsymbol{r}} = \mathfrak{F}(\boldsymbol{q_b}, \dot{\boldsymbol{q}}_b, \boldsymbol{q_l}, \dot{\boldsymbol{q}}_l, \ddot{\boldsymbol{q}}_l)$$
$$\boldsymbol{I}\ddot{\boldsymbol{\theta}} = \mathcal{L}(\boldsymbol{q_b}, \dot{\boldsymbol{q}}_b, \boldsymbol{q_l}, \dot{\boldsymbol{q}}_l, \ddot{\boldsymbol{q}}_l) \quad (4)$$

The optimization algorithm based on GA starts when design parameters, such as the mass and inertias of both the body and legs, are configured together with the locomotion speed V and the average body height h. The GA proceeds by identifying the optimal gait through exploration of various combinations of $\boldsymbol{p}_{GA} = [T, t_i, \beta_i, \boldsymbol{l}_i]$ that are, the parameters characterizing the gait and the thigh-leg geometries, succinctly summarized as vector $\boldsymbol{l}_i$.

In this phase, equations (4) can be approximated under the assumption that the leg trajectory $\boldsymbol{q}_l(\boldsymbol{p}_{GA}, V, h, \boldsymbol{p}_{sp}(x,z), t)$ and its derivatives are autonomous function and preassigned as a function of the assumed gait $\boldsymbol{p}_{GA}$, presuming that the body moves at a constant velocity and height. Moreover, the kinematics of the leg's swing phase relative to the body $\boldsymbol{p}_{sp}(x,z)$ are also predetermined, with a predefined maximum height point to reach, z_{sp}, as schematically depicted in Figure 2. This guarantee to overcome possible obstacles during the motion.

At this point, equations (4) can be easily rewritten in the SRB version with dummy legs, with the additional assumption that body oscillations are small, and that the derivative of the Tait–Bryan angles $\dot{\boldsymbol{\theta}}$ can be reasonably approximated with the angular velocities in the mobile reference frame, resulting in:

$$m\ddot{\boldsymbol{r}} \approx m\boldsymbol{g} + \sum(\boldsymbol{f}_i + \boldsymbol{f}_{l_i})$$
$$\boldsymbol{I}\ddot{\boldsymbol{\theta}} \approx \sum(\boldsymbol{m}_i + \boldsymbol{m}_{l_i}) \quad (5)$$

where $\boldsymbol{g}$ is the gravity acceleration, $\boldsymbol{f}_i$ and $\boldsymbol{m}_i$ represent the forces and moments acting on the body through the contact forces, and similarly denoting $\boldsymbol{f}_{l_i}, \boldsymbol{m}_{l_i}$ for the contributions of the dummy legs.

C. Contact forces constraints

During the contact phase, the legs exert forces with the ground, while no forces are exchanged during the swing phase. This means that, at the start and end of the contact, the forces must be zero. The normal force F_{Z_i} must be strictly positive during the contact, while the longitudinal F_{x_i} and lateral F_{y_i} forces need to obey to the friction law:

$$\sqrt{F_{xi}^2 + F_{yi}^2} \leq \mu_s F_{zi} \quad (6)$$

with μ_s the static friction coefficient.

From the observation of animal locomotion, a typical shape emerges for the longitudinal force. Animals display the habit of always decelerate at the beginning of the contact $\dot{F}_{x_i}(t_i) < 0$ and then accelerate to propel themselves forward $\dot{F}_{x_i}(t_i + T_i) < 0$ and permit the foot detachment, (Figure 2). A similar force trend holds for the lateral force that is responsible for the unavoidable lateral staggering of the quadruped's body.

D. Periodicity constraints and time-averaged values.

To identify a valid locomotion, it is essential to impose the constraint of kinematic periodicity, which means that within one cycle T, the pitch, roll, and yaw movements and their derivatives, as well as the lateral and vertical motion, are equal. For longitudinal motion, it is required to maintain the same starting and ending cycle velocity and to ensure that the average velocity V is respected. For vertical motion, the desired average height is h:

$$\boldsymbol{q}_b(0) = \boldsymbol{q}_b(T) \; with \; x(0) \neq \mathrm{x}(T)$$
$$\dot{\boldsymbol{q}}_b(0) = \dot{\boldsymbol{q}}_b(T)$$
$$V = \frac{1}{T}\int_0^T x(t)dt \quad ; \quad h = \frac{1}{T}\int_0^T z(t)dt \quad (7)$$

II. Optimization algorithm

A. General Outline of the Optimization Algorithm

The algorithm is organized in layers, with a global optimizer represented by the GA. Within the GA, there are subsequent sub-optimizations based on Non-Linear Programming (NLP) and Quadratic Programming (QP) techniques. The overall objective of the GA is to identify the optimal locomotion gait, $\boldsymbol{p}_{GA}$, which minimizes a specific fitness function defined as the sum of two contributions:

- the cost of transport, CoT;
- the jerk of the contact forces $\dot{\boldsymbol{f}}$.

This is achieved while ensuring that the selected solutions always satisfy the motion periodicity conditions described in the previous section.

Once the algorithm converges, it provides the general locomotion solution in which the complete robot dynamics equation (1) is entirely resolved. This includes determining the body trajectory $\boldsymbol{q}_b$, the leg trajectories $\boldsymbol{q}_l$, the joint torques $\boldsymbol{\tau}$, and the ground contact forces $\boldsymbol{f}_i$.

B. First Algorithm Layer: Non-Linear Programming

The first sub-optimizer provides an estimate of the ground-exchanged forces' shape, identifying an approximate solution for the contact forces $\boldsymbol{f}_i$ that satisfy the SRB - dummy legs model as reported in (5). The following actions are then executed sequentially:

1) the GA is initialized by assigning the parameters of the robot to be optimized, including the average velocity and height V, h, as well as the masses, the geometry and inertias of the body;
2) the GA generates a candidate population of parameters $\boldsymbol{p}_{GA}$ for gait type T, t_i, β_i and the lengths of the hip, thigh, and leg links $\boldsymbol{l}_i$;
3) the masses and inertias of the leg links are calculated based on $\boldsymbol{l}_i$;
4) the leg trajectories $\boldsymbol{q}_l, \dot{\boldsymbol{q}}_l, \ddot{\boldsymbol{q}}_l$ are defined using inverse kinematics for the stance phase (CP) and pre-configured Bézier curves for the swing phase (SP). The SP trajectory is constructed so that the foot tip reaches a predetermined height, z_{sp}, representing the clearance of a hypothetical terrain obstacle. The $\boldsymbol{q}_l(t)$ are referred to as dummy legs because they are

attached to a hypothetical body that moves at a constant gait with fixed velocity and height, and they are a function of the optimization vector $\boldsymbol{p}_{GA}$;

5) the forces and moments $\boldsymbol{f}_{l_i}, \boldsymbol{m}_{l_i}$ transmitted by the legs to the body are evaluated based on the previously defined leg trajectories.

At this point, the NLP determines the shape of the ground-reaction forces and the initial conditions of the body $\boldsymbol{q_b}(0), \dot{\boldsymbol{q}}_{\boldsymbol{b}}(0)$ to minimize the jerk of the contact forces. To reduce the number of unknowns in the problem and expedite the method, we have described the forces $\boldsymbol{f}_i$ as functions of k unknown coefficients $\boldsymbol{c}_k$, which, in the interval CP $\in [t_i, T_i]$, describe the spline shape of these forces, resulting in $\boldsymbol{f}_i(\boldsymbol{c}_k)$. Additionally, the NLP must ensure:

i. the non-slipping of the foot when it is in contact with the ground, as reported in equation (8), the positive direction of normal forces, and the braking conditions during the initial contact $\dot{F}_{x_i}(t_i) < 0$ and detachment $\dot{F}_{x_i}(t_i + T_i) < 0$, all synthetically represented by the inequality constraint $\boldsymbol{h}_i(\boldsymbol{c}_k) < 0$;

ii. adherence to the motion equation for SRB dummy legs as stated in (5);

iii. the periodic conditions and time-averaged values discussed in (7) and synthetically represented by $\boldsymbol{w}(\boldsymbol{q}_b(0), \dot{\boldsymbol{q}}_b(0), \boldsymbol{q}_b(\mathrm{T}), \dot{\boldsymbol{q}}_b(\mathrm{T}), V, h) = 0$.

The subproblem is summarized as follows:

$$\begin{aligned} &\min_{\boldsymbol{c_k}, \boldsymbol{q_b}(0), \dot{\boldsymbol{q}}_{\boldsymbol{b}}(0)} \sum_i \int_{t_i}^{T_i} \dot{\boldsymbol{f}}_i(\boldsymbol{c}_k)\, dt \\ &\textit{subject to} \quad \boldsymbol{h}_i(\boldsymbol{c}_k) < 0 \\ &\begin{cases} m\ddot{\boldsymbol{r}} = m\boldsymbol{g} + \sum \left(\boldsymbol{f}_i(\boldsymbol{c}_k) + \boldsymbol{f}_{\boldsymbol{l}_i}\right) \\ \boldsymbol{I}\ddot{\boldsymbol{\theta}} = \sum \left(\boldsymbol{m}_i\left(\boldsymbol{r}, \boldsymbol{f}_i(\boldsymbol{c}_k)\right) + \boldsymbol{m}_{\boldsymbol{l}_i}\right) \end{cases} \\ &\boldsymbol{w}(\boldsymbol{q}_b(0), \dot{\boldsymbol{q}}_b(0), \boldsymbol{q}_b(\mathrm{T}), \dot{\boldsymbol{q}}_b(\mathrm{T}), V, h) = 0 \end{aligned} \tag{8}$$

The NLP assembled in this way is a typical shooting problem, where once the guess $\boldsymbol{c_k}, \boldsymbol{q_b}(0), \dot{\boldsymbol{q}}_{\boldsymbol{b}}(0)$ are identified, the first differential equation of (5) is explicitly solved. At this point, obtaining the translational motion of the body $\boldsymbol{r}$ allows the calculation of the moments that the contact forces exert on the body $\boldsymbol{m}_i(\boldsymbol{r})$, and then proceed with the explicit solution of the second differential equation (5).

Once the NLP minimum problem is solved, the trajectory of the body $\boldsymbol{q}_b = \boldsymbol{q}_{b_{NLP}}$ and the contact forces with the ground $\boldsymbol{f}_i = \boldsymbol{f}_{i_{NLP}}$ are obtained. At this point, it is possible to calculate, again through inverse kinematics, the new leg trajectories $\boldsymbol{q}_l = \boldsymbol{q}_{l_{NLP}}$, this time compatible with the body motion found. The NLP solution is tested in the global motion equation (2), evaluating the residual error of this first solution step as $\boldsymbol{\varepsilon}_{NLP} = \left[\varepsilon_x, \varepsilon_y, \varepsilon_z, \varepsilon_\theta, \varepsilon_\phi, \varepsilon_\psi\right]$.

$$\begin{aligned} \boldsymbol{\varepsilon}_{NLP} = \boldsymbol{M}_b(\boldsymbol{q})\ddot{\boldsymbol{q}}_b + \boldsymbol{C}_b(\boldsymbol{q}, \dot{\boldsymbol{q}})\dot{\boldsymbol{q}}_b - \boldsymbol{g}_b(\boldsymbol{q}_b) - \boldsymbol{J}_b(\boldsymbol{q})^T\boldsymbol{f} \\ - \boldsymbol{\mathcal{R}}_b(\boldsymbol{q}, \dot{\boldsymbol{q}}, \ddot{\boldsymbol{q}}_l) \end{aligned} \tag{9}$$

By using equation (3), it is also possible to evaluate the control action torques $\boldsymbol{\tau}$ that enable the assessment of the CoT_{NLP}.

In the work [10], the authors proposed an optimization model similar to the first algorithmic step, which has been expanded and solved here using a different methodology, the NLP. In [10], they computed the CoT_{NLP}, assuming that the robot has negligible leg masses. However, in this context, the same authors demonstrate how the CoT_{NLP} can deviate when considering leg masses. The algorithm presented here not only allows for the optimization of CoT but also enables its minimization in the presence of legs with masses, consistently achieving periodic gaits. This is achieved by fully solving the multi-body motion equations (1), resulting in an $\boldsymbol{\varepsilon}$ equal to zero.

C. Second Algorithm: Enhancing the Optimization Series with QP

The second part of the algorithm involves the detailed solution of the contact forces $\boldsymbol{f}_i$, which now directly satisfy the motion equation (2). The $\boldsymbol{f}_{i_{NLP}}$ previously found serve as guesses for the following new programming problem, with the difference that now the $\boldsymbol{f}_i$ are discretized in time within the interval $[0; T]$. The new minimum problem is addressed by means of a QP approach, with the aim of minimizing the ground contact forces

exchanged while ensuring that the multi-body motion equations (2) are satisfied along the trajectories obtained from the NLP, $\boldsymbol{q}_{b_{NLP}}$ and $\boldsymbol{q}_{l_{NLP}}$:

$$\begin{aligned} &\min_{\boldsymbol{f}_i} \sum \frac{1}{2}\boldsymbol{f}_i^T\boldsymbol{\mathcal{H}}\boldsymbol{f}_i + \boldsymbol{\mathcal{F}}^T\boldsymbol{f}_i \\ &\textit{subject to} \quad \boldsymbol{A}\boldsymbol{f}_i \leq \boldsymbol{b} \\ &\boldsymbol{M}_b(\boldsymbol{q})\ddot{\boldsymbol{q}}_b + \boldsymbol{C}_b(\boldsymbol{q}, \dot{\boldsymbol{q}})\dot{\boldsymbol{q}}_b \\ &\qquad = \boldsymbol{g}_b(\boldsymbol{q}_b) + \boldsymbol{J}_b(\boldsymbol{q})^T\boldsymbol{f} \\ &\qquad + \boldsymbol{\mathcal{R}}_b(\boldsymbol{q}, \dot{\boldsymbol{q}}, \ddot{\boldsymbol{q}}_l) \end{aligned} \tag{10}$$

where the matrix $\boldsymbol{\mathcal{H}}$ and the vector $\boldsymbol{\mathcal{F}}$ are generical gains of the objective function; the matrix $\boldsymbol{A}$ and vector $\boldsymbol{b}$ are defined to satisfy the linearized friction constraint, select positive normal forces during CP and the incipient braking and detachment conditions $\dot{F}_{x_i}(t_i) < 0$ and $\dot{F}_{x_i}(t_i + T_i) < 0$. The equality constraints make it possible to achieve a new residual error $\boldsymbol{\varepsilon}_{QP}$ less then the previous $\boldsymbol{\varepsilon}_{NLP}$, using the kinematic solution of the body $\boldsymbol{q}_{b_{NLP}}$ and legs $\boldsymbol{q}_{l_{NLP}}$ found by the first optimization algorithm.

D. Evaluation of the GA's constraint and fitness function

At this point, we move on to assess the constraint equation of the GA, specifically, evaluating if the periodicity conditions are met. To do this, we take the $\boldsymbol{f}_{i_{QP}}$ calculated from the QP and the initial conditions $\boldsymbol{q}_{b_{NLP}}(0), \dot{\boldsymbol{q}}_{b_{NLP}}(0)$ found by the NLP, and we check the gait periodicity $\boldsymbol{w}(\boldsymbol{q}_b(0), \dot{\boldsymbol{q}}_b(0), \boldsymbol{q}_b(\mathrm{T}), \dot{\boldsymbol{q}}_b(\mathrm{T}), V, h) = 0$ by solving explicitly the equation (2). At each time step the inverse kinematics is computed to describe leg movement that is compatible with the body. This step allows us to minimize residual errors $\boldsymbol{\varepsilon}$ and evaluate how well the periodicity conditions have been met.

Table 1. Simulation setting parameters.

Parameter	Value	Unit
$[m; V; h]$	$[25; 1; 0.5]$	$[kg; m/s; m]$
$[I_x; I_y; I_z]$	$[0.35; 2.1; 2.1]$	$kg\ m^2$
$[L, W, H]$	$[0.6; 0.25; 0.2]$	m
z_{sp}	0.25	m
$\boldsymbol{l}_i$	$[0.06; 0.33; 0.33]$	m
$\boldsymbol{m}_{leg}$	$[0.06; 0.16; 0.16]$	kg
$\boldsymbol{I}_{hip}$	$[0.01; 0.02; 0.02]$	$kg\ m^2$
$\boldsymbol{I}_{thigh} = \boldsymbol{I}_{calf}$	$[0.03; 0.09; 0.09]$	$kg\ m^2$
$t_{FR} = t_{HL}$	0	s
$t_{HR} = t_{FL}$	0.23	s

Similarly to what was done before, from equation (3), it is now possible to calculate the control actions $\boldsymbol{\tau}$ expended. At this point, we proceed with the evaluation of the GA's fitness function that we aim to minimize, which is a function that sums the CoT and the jerk of the contact forces:

$$J = \frac{1}{mgdT}\int_0^T |\boldsymbol{\tau}\cdot\dot{\boldsymbol{q}}_l|\,dt + \frac{1}{T}\int_0^T \|\dot{\boldsymbol{f}}\|\,dt \qquad (11)$$

with d being the distance travelled by the robot in a complete cycle with a period T.

III. Results and Discussion

In this paper, we aim to demonstrate how the optimization algorithm, as assembled, can quickly and easily identify fully closed solutions that adhere to periodicity. We tasked the GA with minimizing the fitness function of a trotting gait that does not exhibit support polygons but only alternate support lines (Figure 1). This type of configuration is achieved by setting a duty factor $\beta_{FR} = \beta_{FL} = 0.5$ and $\beta_{HR} = \beta_{HL} = 0.5$ for both the front and rear legs and ensuring that there is no overlap between the pair HL, FR with HR, FL. Unlike the classic walking trot, which is characterized by the presence of a support polygon, the trot or flying trot are gaits that are often discarded in robotics due to their complexity to execute [9] and do not allow chance for errors.

Table 1 presents the robot's data, where it has been required that the leg length $\boldsymbol{l}_i$, as well as their mass $\boldsymbol{m}_{leg}$ and inertia of each link ($\boldsymbol{I}_{hip}, \boldsymbol{I}_{thigh}, \boldsymbol{I}_{calf}$), be the same for each $i-th$ leg. The measurements for $\boldsymbol{l}_i$ and $\boldsymbol{m}_{leg}$ are organized as $[hip, thigh, calf]$. The inertias are centered at the joint and ordered such that the first component is aligned with the cylindrical axis, and the other two are the same because the link is axially symmetric. The sum of the masses of all leg links accounts for approximately 6% of the body mass, inspired by the robot presented in [1]. In Figure 3, the forces and moments that various sub-optimizers have found for identifying the global solution of the GA are shown. In particular, the black line indicates the solution found by NLP using the SRB with dummy legs, for which $\boldsymbol{f}_{i_{NLP}}$ e $\boldsymbol{m}_{i_{NLP}}$ are

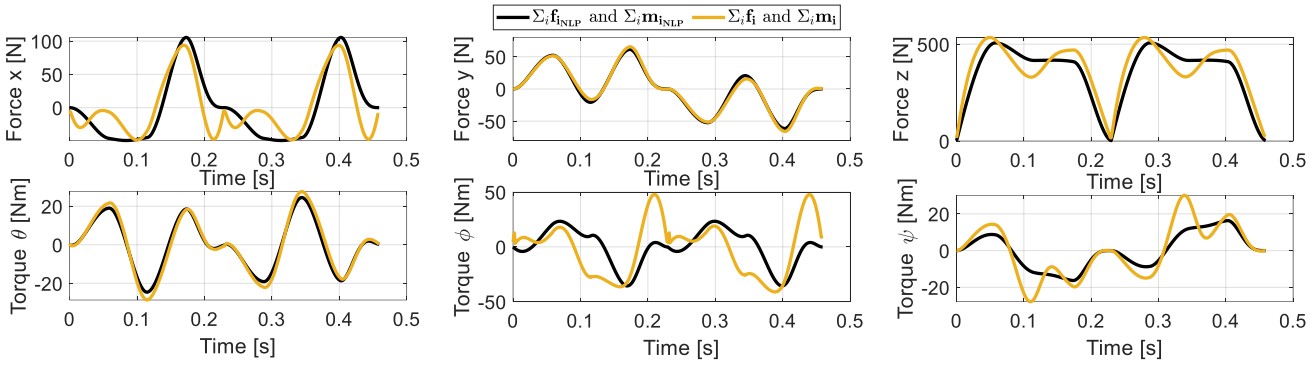

Figure 3: Optimization results. The black lines represent the forces and torques that result after the non-linear programming. The yellow lines represent the forces and torques of the final solution of the algorithm.

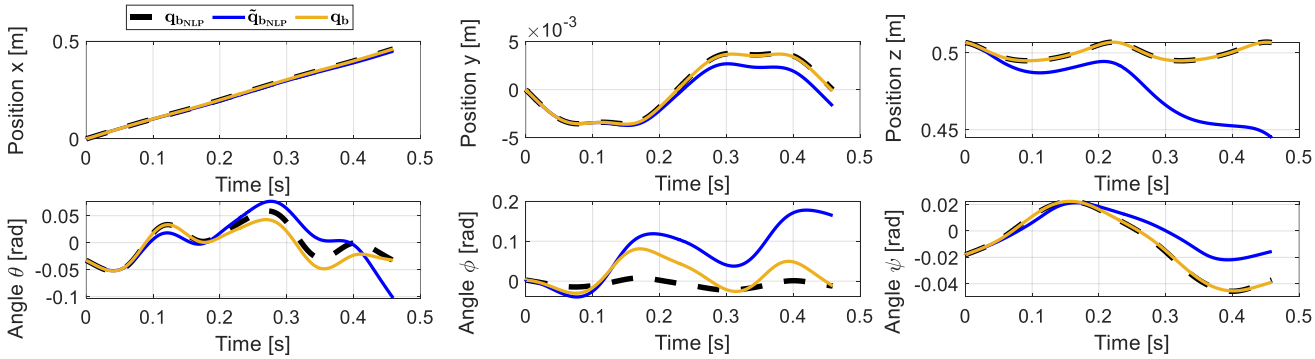

Figure 4: Optimization results: the black lines represent the body motion $\boldsymbol{q}_{b_{NLP}}$ after the solution of the NLP; the blue lines represent the body motion $\tilde{\boldsymbol{q}}_{b_{NLP}}$ found by straight forwarding the multi-body equations; the yellow represent the final trotting gait $\boldsymbol{q}_b$.

reported. In yellow, the final solution's $\boldsymbol{f}_i$ and $\boldsymbol{m}_i$ are shown. In Figure 4, the body's kinematics are presented, with the dashed black line representing $\boldsymbol{q}_{b_{NLP}}$, while the blue line represents the solution related to the first NLP sub-optimizer, obtained when the results of the forces $\boldsymbol{f}_{i_{NLP}}$, $\boldsymbol{q}_{l_{NLP}}$ and $\boldsymbol{q}_{b_{NLP}}(0)$ $\dot{\boldsymbol{q}}_{b_{NLP}}(0)$ are used to evaluate the explicit solution of the multi-body motion equations (2). Thus, $\tilde{\boldsymbol{q}}_{b_{NLP}}$, due to the presence of $\boldsymbol{\varepsilon}_{NLP}$, does not comply with the periodicity conditions and diverges. In yellow, the final solution $\boldsymbol{q}_b$ calculated from the explicit solution of (2) based on $\boldsymbol{f}_{i_{QP}}$, while maintaining $\boldsymbol{q}_{l_{NLP}}$ and the initial conditions found by the NLP $\boldsymbol{q}_{b_{NLP}}(0)$, $\dot{\boldsymbol{q}}_{b_{NLP}}(0)$.

The trajectories $\boldsymbol{q}_b$, compared to the trajectories $\boldsymbol{q}_{b_{NLP}}$, imply an increase in the CoT value ($\approx$ 5% more) or, in other words, to a higher effort of the actuation system in applying the torques $\boldsymbol{\tau}$ to the robot joints. It's important to emphasize that even though the solution of an NLP may find a low CoT, on the other hand, the dynamic solution is no longer compatible with non-negligible leg masses.

IV. Conclusion

This article represents a significant improvement of the current optimization techniques used to generate gaits of quadruped robots. The models used to date do not consider the dynamics of the legs and the effects they have on the robot's body. The algorithm presented here is able to select solutions for complex and weakly controllable gaits, such as trotting without a support polygon. The algorithm not only finds solutions compatible with nonlinear dynamics but also selects those that minimize energy cost. All of this is made possible through a stepwise solution approach where each intermediate solution serves as the guess for the next algorithm.

Future developments will focus on analyzing the stability and robustness of the gaits identified under conditions of uncertain parameters such as mass distribution or terrain roughness.

References

[1] G. Bledt, J. Powell, B. Katz, J. Di Carlo, P. M. Wensing, and S. Kim, "MIT Cheetah 3: Design and Control of a Robust, Dynamic Quadruped Robot," presented at the IEEE/RSJ International Conference on Intelligent Robots and Systems (IROS), Madrid, Spain, 2018.

[2] M. Focchi, A. del Prete, and I. Havoutis, "High-slope terrain locomotion for torque-controlled quadruped robots," *Auton Robot,* vol. 41, pp. 259-272, 2017.

[3] A. W. Winkler, F. Farshidian, M. Neunert, D. Pardo, and J. Buchli, "Online walking motion and foothold optimization for quadruped locomotion," in *2017 IEEE International Conference on Robotics and Automation (ICRA)*, 29 May-3 June 2017 2017, pp. 5308-5313.

[4] A. W. Winkler, F. Farshidian, D. Pardo, M. Neunert, and J. Buchli, "Fast Trajectory Optimization for Legged Robots Using Vertex-Based ZMP Constraints," *IEEE Robotics and Automation Letters,* vol. 2, no. 4, pp. 2201-2208, 2017.

[5] A. W. Winkler, C. D. Bellicoso, M. Hutter, and J. Buchli, "Gait and Trajectory Optimization for Legged Systems Through Phase-Based End-Effector Parameterization," *IEEE Robotics and Automation Letters,* vol. 3, no. 3, pp. 1560-1567, 2018.

[6] X. Meng, S. Wang, Z. Cao, and L. Zhang, "A Review of Quadruped Robots and Environment Perception," presented at the 35th Chinese Control Conference, Chengdu, China, 2016.

[7] K. Hashimoto *et al.*, "A four-limbed disaster-response robot having high mobility capabilities in extreme environments," in *2017 IEEE/RSJ International Conference on Intelligent Robots and Systems (IROS)*, 24-28 Sept. 2017 2017, pp. 5398-5405.

[8] T. Matsuzawa *et al.*, "Crawling and foot trajectory modification control for legged robot on uneven terrain," *International Journal of Mechatronics and Automation,* vol. 7, p. 1, 01/01 2020.

[9] J. He and F. Gao, "Mechanism, Actuation, Perception, and Control of Highly Dynamic Multilegged Robots: A Review," *Chinese Journal of Mechanical Engineering,* vol. 33, no. 1, p. 79, 2020/11/09 2020.

[10] G. Pepe, M. Lauernza, N. P. Belfiore, and A. Carcaterra, "Quadrupedal Robots' Gaits Identification via Contact Forces Optimization," *Appl. Sci.,* vol. 11, 2102, 2021, doi: https://doi.org/10.3390/app11052102.

[11] M. Laurenza, G. Pepe, and A. Carcaterra, "Gait Optimization Method for Quadruped Locomotion," in *Advances in Nonlinear Dynamics*, Cham, W. Lacarbonara, B. Balachandran, M. J. Leamy, J. Ma, J. A. Tenreiro Machado, and G. Stepan, Eds., 2022// 2022: Springer International Publishing, pp. 439-449.

[12] D. Gong, J. Yan, and G. Zuo, "A Review of Gait Optimization Based on Evolutionary Computation," *Applied Computational Intelligence and Soft Computing,* vol. 2010, p. 413179, 2010/06/24 2010.

[13] T. Kato, K. Shiromi, M. Nagata, H. Nakashima, and K. Matsuo, "Gait pattern acquisition for four-legged mobile robot by genetic algorithm," presented at the IECON 2015 - 41st Annual Conference of the IEEE Industrial Electronics Society, Yokohama, Japan, 2015.

[14] M. Schwenzer, M. Ay, T. Bergs, and D. Abel, "Review on model predictive control: an engineering perspective," *The International Journal of Advanced Manufacturing Technology,* vol. 117, no. 5, pp. 1327-1349, 2021/11/01 2021.

[15] A. Zanotti, M. Laurenza, G. Pepe, and A. Carcaterra, "The role of spine elasticity on legged locomotion," presented at the Eurodyn 2023, Delft, The Netherlands, 2023. [Online]. Available: https://hdl.handle.net/11573/1686581.

[16] E. Koco and Z. Kovacic, "Multiobjective Locomotion Optimization of Quadruped Robot with Different 2DOF Configurations of Actuated Spine," presented at the 2016 24th Mediterranean Conference on Control and Automation (MED), Athens, Greece, 2016.

[17] Q. Deng, S. Wang, W. Xu, J. Mo, and Q. Liang, "Quasi passive bounding of a quadruped model with articulated spine," *Mechanism and Machine Theory,* vol. 52, pp. 232-242, 2012.

[18] U. Culha and U. Saranli, "Quadrupedal bounding with an actuated spinal joint," presented at the 2011 IEEE International Conference on Robotics and Automation, Shanghai, China, 2011.

[19] A. J. Ijspeert, "Central pattern generators for locomotion control in animals and robots: A review," *Neural Networks,* vol. 21, no. 4, pp. 642-653, 2008/05/01/ 2008.

[20] W.-L. Ma, K. Akbari Hamed, and A. Ames, *First Steps Towards Full Model Based Motion Planning and Control of Quadrupeds: A Hybrid Zero Dynamics Approach*. 2019, pp. 5498-5503.

[21] J. D. Carlo, P. M. Wensing, B. Katz, G. Bledt, and S. Kim, "Dynamic Locomotion in the MIT Cheetah 3 Through Convex Model-Predictive Control," in *2018 IEEE/RSJ International Conference on Intelligent Robots and Systems (IROS)*, 1-5 Oct. 2018 2018, pp. 1-9.